American Mineralogist, Volume 89, pages 759–766, 2004

Magmatic srilankite (Ti_2ZrO_6) in gabbroic vein cutting oceanic peridotites: An unusual product of peridotite-melt interactions beneath slow-spreading ridges

TOMOAKI MORISHITA,[1,*] JINICHIRO MAEDA,[2] SUMIO MIYASHITA,[3] TAKESHI MATSUMOTO,[4,†] AND HENRY J. B. DICK[5]

[1]Graduate School of Natural Science and Technology, Kanazawa University, Kanazawa 920-1192, Japan
[2]Graduate School of Science, Hokkaido University, Hokkaido 060-0810, Japan
[3]Department of Geology, Faculty of Science, Niigata University, Niigata 950-2181, Japan
[4]Marine Science Department, Nippon Marine Enterprises, Ltd., Yokosuka 238-0004, Japan
[5]Department of Geology and Geophysics, Woods Hole Oceanographic Institution, Woods Hole, Massachusetts 02543, U.S.A.

ABSTRACT

We report srilankite in a gabbroic vein cutting a serpentinized peridotite collected from the Atlantis II Fracture Zone, the slow-spreading Southwest Indian Ridge, using submersible SHINKAI 6500 of the Japanese Marine Science Technology Center. Srilankite occurs in small patches, <30 μm across, always coexisting with ilmenite and rutile. Zircon, apatite, and phlogopite also occur as accessory minerals in the vein. The Zr/Ti ratio of the srilankite is close to the stoichiometric value of one-half ($Ti_{2.00}Zr_{0.98}Hf_{0.01}Fe_{0.01}O_6$). Based on petrography, the srilankite appears to have co-crystallized with ilmenite and rutile from melts rather than through metamorphic recrystallization. Mineral assemblages and mineral compositions in the vein indicate that melts that produced the vein have high concentrations of compatible elements (MgO and Cr_2O_3) as well as incompatible elements (high-field strength elements, K_2O, and H_2O). On the other hand, TiO_2-enrichment of minerals in the peridotite host on the periphery of the gabbroic vein may have resulted from interaction with the melts. Geochemical interactions between peridotite and melt in the upper mantle may effectively concentrate incompatible elements in a modified melt, which may precipitate srilankite directly. Physical conditions under slow-spreading ridges, characterized by a highly attenuated magma supply and high rock/melt ratio, favor peridotite-melt interactions.

INTRODUCTION

Srilankite (Ti_2ZrO_6) having the orthorhombic α-PbO_2 structure was originally described in pebbles in the washing concentrate of a gemstone mine in Rakwana in the province of Sabaragamuva, Sri Lanka (Willgallis et al. 1983). It was also reported as inclusions in garnets from the Yagodka lamprophyre pipe in Tobuk-Khatystyr field (Kostrovitskiy et al. 1993), and from Colorado Plateau ultramafic diatremes in the Navajo Volcanic Field (Wang et al. 1999). Wang et al. (1999) suggested that srilankite and other oxide inclusions in garnets from the latter were formed from a fluid/melt phase, probably a Mg-rich and SiO_2-undersaturated melt. Recently, Bingen et al. (2001) reported srilankite from crustal mafic granulite and interpreted it as a reaction product between baddeleyite and ilmenite controlled by very local conditions where no free silica was available. Thus, the occurrence of srilankite is an indicator of the high HFSE (high field strength elements)/SiO_2 conditions required for its formation. We have found srilankite in a gabbroic vein cutting a serpentinized peridotite collected from the Atlantis II Fracture Zone, the slow-spreading Southwest Indian Ridge (SWIR). Here, we report the occurrence and chemical compositions of this srilankite, and discuss its origin to provide insight on magmatic processes occurring beneath slow-spreading ridges.

* E-mail: moripta@kenroku.kanazawa-u.ac.jp
† Present address: Faculty of Science, University of the Ryukyus, Okinawa 903-0213, Japan.

GEOLOGICAL BACKGROUND AND SAMPLE DESCRIPTION

The studied sample was collected at 2605 m depth from an outcrop exposed on the eastern rift valley wall of the Atlantis II Fracture Zone, the SWIR (Fig. 1), during Dive no. 643 of the ABECE cruise using submersible SHINKAI 6500 of the Japan Marine Science Technology Center (JAMSTEC). The SWIR is a slow-spreading ridge with a 14 mm/year full-spreading rate (Hosford et al. 2003). The Atlantis II Fracture Zone is a 199 km offset of the SWIR with a 6 km deep transform-valley. Hole 735 B of the Ocean Drilling Program (Legs 118 and 176), which succeeded in recovering an almost complete 1.5 km section of gabbroic rocks originally formed at the axis of the SWIR (e.g., Dick et al. 2000), is at Atlantis Bank, located 100 km south of the SWIR rift valley on the crest of the eastern traverse ridge of the Atlantis II Fracture Zone. Dive no. 643 was carried out along a steep cliff on the southeastern wall of Atlantis Bank. Crustal thickness measured away from the transform east of Hole 735B and near the Indian Ocean Triple Junction ranges from 4 to 5 km (Bown and White 1994; Muller et al. 1997, 1999). Drilling at Hole 735B did not reach ultramafic rock, but a dredged sample from the Atlantis II Fracture Zone indicates that peridotite is probably present within a few hundred meters of the bottom of the Hole (Natland and Dick 2001). Seismic Moho at Hole 735B is, however, estimated to be 5 km below the sea floor, and is interpreted as an alteration front of partially serpentinized peridotite (Muller et al. 1997; Dick et al. 2000;

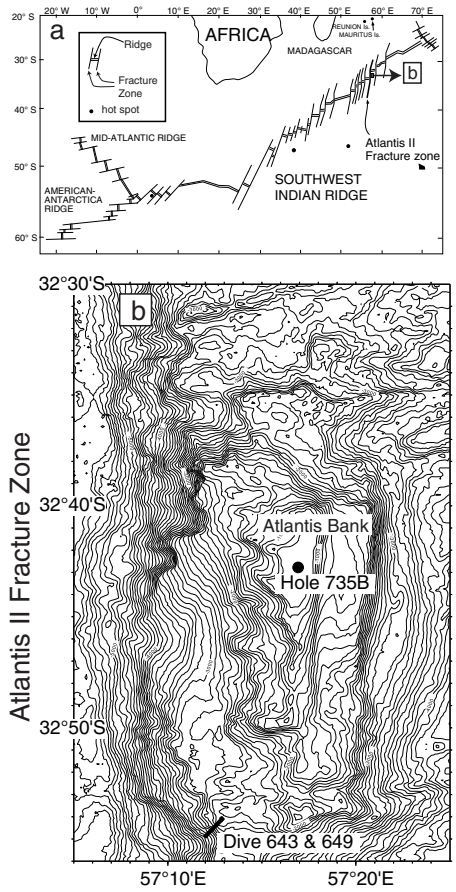

FIGURE 1. (**a**) Location of the study area on the Southwest Indian Ridge; portions of the Mid-Atlantic Ridge and American-Antarctica Ridge also shown. (**b**) Bathymetric map of the Atlantis Bank region adjacent to the Atlantis II Fracture Zone. Dive trace of no. 643 (including no. 649) is the location from which the studied sample was collected. The site of Hole 735B of the Ocean Drilling Program is also shown.

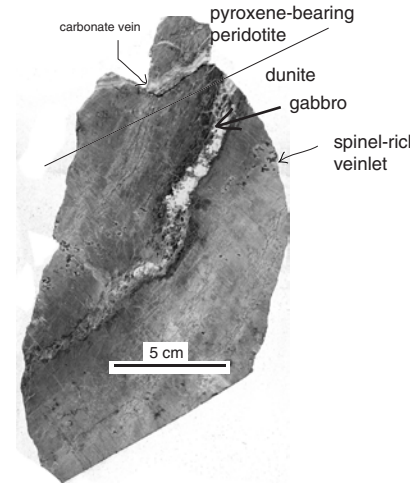

FIGURE 2. Sawed surface of the studied sample. Note that the direction of the spinel-rich veinlet is concordant with lithological boundary between the dunite and the two-pyroxene peridotite, and that the layered structure is cut by gabbroic vein.

Natland and Dick 2001).

Thirteen serpentinized peridotites and 2 gabbros were collected during Dive no. 643. All gabbros were collected from recent talus, whereas 8 peridotites were collected from an outcrop or on an outcrop. This result indicates that the area along the dive track mainly consists of serpentinized peridotite. Moreover, we also confirmed by another dive (Dive no. 649) that gabbros are exposed of 2561 to 2493 m depth along an extended track from Dive no. 643 (Fig. 1). Almost all peridotite samples are lherzolite except for the studied sample.

The studied sample (643R15) mainly consists of dunite with a small amount of dunitic lherzolite at the edge of the sample, and is extensively serpentinized and weathered (Fig. 2). No relics of olivine have been found in the sample. There is a chromian spinel-rich vein, 1 cm in thickness, in the dunite lying parallel to the lithological boundary between the dunite and dunitic lherzolite that imparts a layered structure to the sample (Fig. 2). Clinopyroxene in the dunite forms a symplectitic intergrowth with vermicular chromian spinel (called cpx-spl symplectite hereafter) but no orthopyroxene has been found in the intergrowths. The cpx-spl symplectite is sporadically distributed in the matrix. In addition to the cpx-spl symplectite, spinel also occurs as rounded anhedral discrete grains, up to 5 mm across.

Olivine textures are difficult to identify due to complete serpentinization and weathering. The dunitic lherzolite has a protogranular texture. Evidence from pyroxene textures indicates weak deformation of the peridotite host, suggesting that the layered structure in the peridotite host is a primary magmatic feature that was modified by slight low-temperature deformation, i.e., the dunite occurred as a dike in the dunitic lherzolite host. A gabbroic vein, 1.5 cm in thickness, obliquely cuts the igneous layering of the peridotite host (Fig. 2).

The gabbroic vein is also extensively altered and cut by many carbonate veins. It is, therefore, generally difficult to distinguish the primary magmatic phases in the vein. Despite secondary alteration and/or metamorphism, this study focuses on igneous processes. Orthopyroxene having anhedral granular shape (up to 4 mm) with weak wavy extinction is the main primary igneous phase remaining (Fig. 3a). Orthopyroxene may tend to be more abundant at the margin than the middle of the vein. A few anhedral clinopyroxene grains are present. Exsolution lamellae are common in both orthopyroxene and clinopyroxene. From the texture of pyroxenes, the gabbroic vein may have also suffered limited plastic deformation. Small amounts of olivine, now completely serpentinized, locally are associated with orthopyroxene. No relics of the primary magmatic plagioclase remain. Opaque minerals (rutile, ilmenite, zircon, and srilankite), apatite, and phlogopite are accessory minerals in the vein. No magnetite has been found. The modal proportions of carbonate minerals, gabbroic material (except for opaque minerals), and opaque minerals were measured in an area of about 1.5×1 cm with an interval of 0.2 mm by a point-counting (total 3501 counts), and are 53, 46, and <1 (0.6) vol%, respectively. Despite its smallness, this area represents a typical texture of the gabbroic vein based on visual estimate under microscope. Modal abundances of opaque minerals, thus, might be <2% in the gabbroic portion. Srilankite is rare

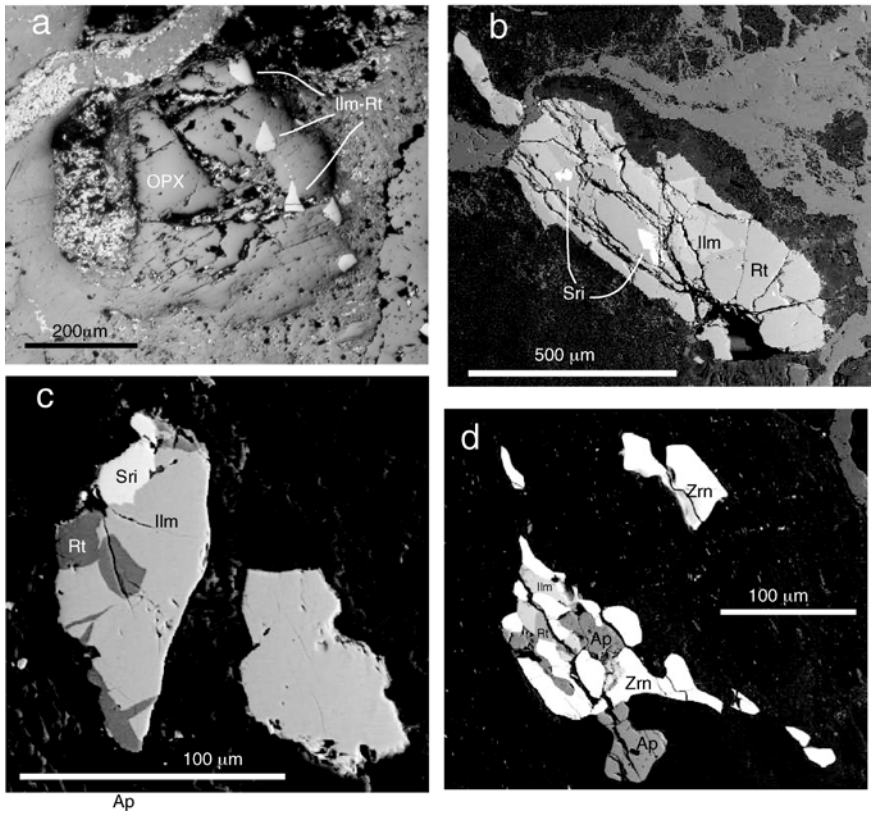

FIGURE 3. Photomicrographs of the studied gabbroic vein. (**a**) A reflected light image of granular orthopyroxene in the gabbroic vein. Some ilmenite-rutile grains are included in the orthopyroxene. (**b**) and (**c**) Back-scattered electron images of srilankite-rutile-ilmenite grains. Note that srilankite occurs as small rounded to prismatic grains inside (**b**) as well as at the margin (**c**) of ilmenite-rutile grains. (**d**) Back-scattered electron image of a zircon-ilmenite-rutile-apatite grain. Note that zircons also occur as discrete grains. OPX = orthopyroxene, Ilm = ilmenite, Rt = rutile, Sri = srilankite, Zrn = zircon, and Ap = apatite.

and occurs as small rounded to prismatic grains, up to 30 μm in size, at the margin and/or inside of ilmenite-rutile grains ranging from sub-millimeter to 1.5 mm across (Figs. 3b, 3c). Srilankite tends to be found within an area rich in orthopyroxene grains. Ilmenite-rutile grains locally are included in orthopyroxene (Fig. 3a). Zircon and apatite occur as individual grains or intergrown with ilmenite and rutile (Fig. 3d). It is noteworthy that zircon never has been found from an area where srilankite-bearing ilmenite-rutile grains occur in the thin section. Rare phlogopite is present, and is associated with ilmenite-rutile grains.

MINERAL CHEMISTRY

Methods

Mineral compositions were analyzed with a JEOL JXA-8800 Superprobe at the Center for Cooperative Research of Kanazawa University. The analyses were performed with an accelerating voltage of 15–20 kV and a beam current of 15–20 nA using a 1–3 μm diameter beam. X-ray peaks were counted for 10 to 100 s, and both high and low backgrounds were measured. JEOL software using ZAF corrections was also employed. The following standards were used: quartz = Si; $KTiPO_4$ = K and Ti; rutile = Ti (in opaque oxides); corundum = Al; eskolaite = Cr; fayalite = Fe; manganosite = Mn; periclase = Mg; wollastonite = Ca; jadeite = Na; nickel oxide = Ni, niobium metal = Nb; tantalum metal = Ta; cubic zirconia = Zr and Hf. Representative analyses of the primary minerals in the dunite and gabbroic vein are shown in Tables 1 and 2.

Dunite

The Mg' [= Mg/(Mg + Fe_T) atomic ratio] of clinopyroxene in the dunite shows only a small variation (0.91–0.92), some of which is due in part to subsolidus Mg-Fe redistribution that depends on the relative amount of clinopyroxene (e.g., Arai et al. 1988). The TiO_2 content of clinopyroxene is 0.2 wt% except near the gabbroic vein. However, clinopyroxene near the gabbroic vein is enriched in TiO_2, up to 1 wt% (Table 1).

The Cr' [= Cr/(Cr + Al) atomic ratio] and TiO_2 content of spinel in the dunite are usually homogeneous in the dunite irrespective of the differences in shape, and are 0.3 and 0.1 wt%, respectively (Fig. 4). However, the Cr' and TiO_2 content of spinel near the gabbroic vein are high, up to 0.5 and 1.5 wt%, respectively (Fig. 4).

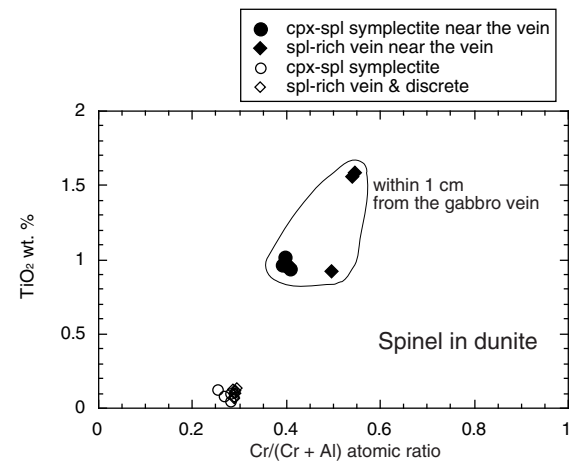

FIGURE 4. The Cr' [=Cr/(Cr + Al) atomic ratio] vs. wt% TiO_2 of spinels in the dunite host. Spl-rich vein = spinel in spinel-rich vein in the studied sample.

TABLE 1. Representative compositions of silicate minerals and spinels in the dunite host and gabbro vein

	Dunite														
	cpx								spl						
	symp cpx		high-Ti symp		spl-rich vein		discrete		high-Ti symp			spl-rich vein near gabbro			
	avg	std no. 5	avg	std no. 4	avg	std no. 7	ave.	std no. 7	R15-4-9	R15-4-10	R-15-4-12	R-15-4-82	R-15-4-85	R15-4-87	R15-4-88
SiO_2	51.95	0.20	52.05	0.35	0.02		0.04		0.06	0.08	0.06	0.01	0.00	0.02	0.09
TiO_2	0.24	0.01	0.92	0.10	0.10	0.03	0.08	0.03	0.92	1.56	1.58	0.94	0.96	0.95	1.01
Al_2O_3	4.37	0.32	3.65	0.43	41.26	0.49	41.87	0.77	26.56	23.19	22.60	32.02	33.61	33.11	33.41
Cr_2O_3	1.13	0.08	1.20	0.11	25.31	0.32	23.29	1.27	38.95	40.79	40.49	33.16	32.43	33.50	32.73
FeO*	2.49	0.23	2.80	0.05	14.92	0.71	16.95	0.72	20.16	21.79	23.23	17.54	17.56	17.49	17.06
MnO	0.06	0.01	0.10	0.01	0.18	0.04	0.15	0.05	0.31	0.31	0.30	0.24	0.21	0.22	0.22
MgO	15.58	0.25	16.21	0.23	17.73	0.24	16.66	0.69	11.69	11.15	10.33	14.04	14.91	15.34	14.31
CaO	24.24	0.41	23.33	0.27	0.01		0.03		0.09	0.13	0.08	0.04	0.00	0.00	0.00
Na_2O	0.61	0.05	0.69	0.04	0.02		0.02		0.01	0.00	0.01	0.03	0.00	0.02	0.00
K_2O	0.02		0.01		0.02		0.01		0.02	0.02	0.01	0.01	0.01	0.00	0.01
NiO	0.03		0.04		n.a.		n.a.		0.15	0.16	0.15	0.18	0.19	0.16	0.15
Total	100.72	0.28	101.02	0.32	99.55	0.82	99.09	1.05	98.90	99.18	98.84	98.19	99.88	100.80	99.00
O=	6		6		4		4		4	4	4	4	4	4	4
Si	1.886	0.009	1.885	0.010	0.001		0.001		0.002	0.002	0.002	0.000	0.000	0.001	0.003
Ti	0.006	0.000	0.025	0.003	0.002	0.001	0.002	0.001	0.021	0.037	0.038	0.021	0.021	0.021	0.023
Al	0.187	0.014	0.156	0.018	1.368	0.009	1.400	0.032	0.968	0.859	0.847	1.132	1.160	1.135	1.163
Cr	0.032	0.002	0.034	0.003	0.563	0.005	0.522	0.025	0.952	1.014	1.018	0.786	0.751	0.770	0.764
Fe*	0.076	0.007	0.085	0.002	0.351	0.017	0.402	0.018	0.521	0.573	0.618	0.440	0.430	0.425	0.421
Mn	0.002	0.000	0.003	0.000	0.004	0.001	0.003	0.001	0.008	0.008	0.008	0.006	0.005	0.005	0.006
Mg	0.843	0.014	0.875	0.013	0.743	0.011	0.704	0.024	0.538	0.522	0.489	0.628	0.651	0.665	0.629
Ca	0.943	0.015	0.905	0.008	0.000		0.001		0.003	0.004	0.003	0.001	0.000	0.000	0.000
Na	0.043	0.003	0.049	0.003	0.001		0.001		0.001	0.000	0.001	0.002	0.000	0.001	0.000
K	0.001		0.001		0.001		0.001		0.001	0.001	0.000	0.000	0.000	0.000	0.000
Ni	0.001		0.001		n.a.		n.a.		0.004	0.004	0.004	0.004	0.005	0.004	0.004
Total	4.020	0.002	4.019	0.003	3.033	0.004	3.037	0.005	3.018	3.025	3.028	3.021	3.023	3.026	3.012
Mg no.	0.918	0.007	0.912	0.002	0.735	0.011	0.696	0.023	0.527	0.503	0.470	0.613	0.635	0.648	0.616
Cr no.	0.148	0.002	0.181	0.013	0.291	0.002	0.272	0.014	0.496	0.541	0.546	0.410	0.393	0.404	0.397
Fe^{3+} no.					4.123	0.585	4.679	0.562	1.954	2.948	3.418	2.245	2.814	3.238	1.439

Notes: Numbers next to S.D.' mean standard deviation and number of analyses. symp = symplectitc aggregate of clinopyroxene and spinel, cpx = clinopyroxene, spl-rich vein = spinel in spinel-rich vein in the studied rock, spl = spinel, opx = orthopyroxene, phl = phlogopite, ave. = average, std = standard deviation, n.a. = not analyzed, FeO* = total iron as FeO, Fe* = total iron as Fe, Mg′ = Mg/(Mg + Fe*) atomic ratio except for spinel (Mg′ for spinel in which Fe^{2+} was calculated from spinel stoichiometry after all Ti was combined with Fe as the ulvöspinel component, Fe_2TiO_4), Cr′ = Cr/(Cr + Al) atomic ratio, $Fe^{3+}{}' = 100 \times Fe^{3+}/(Al + Cr + Fe^{3+})$.

TABLE 2. Chemical compositions of opaque minerals in the gabbo vein

	Srilankite		Zircon		Rutile			ilmenite		
	average	std no. 5	average	std no. 6	Cr, Nb-rich	Zr-rich	Cr-poor	High-Mg	Middle-Mg	Low-Mg
Nb_2O_5	<0.2		<0.2		0.47	<0.2	<0.2	<0.2	<0.2	<0.2
Ta_2O_5	<0.2		<0.2		<0.2	<0.2	<0.2	<0.2	<0.2	<0.2
SiO_2	<0.02		34.69	0.38	0.06	<0.02	<0.02	<0.02	0.03	0.04
TiO_2	56.06	0.34	0.07	0.08	96.15	96.09	96.93	57.71	55.15	53.63
ZrO_2	42.51	0.82	62.95	1.07	0.68	1.82	1.39	<0.1	<0.1	<0.1
HfO_2	0.54	0.07	1.43	0.20	0.07	0.06	<0.05	<0.05	<0.05	<0.05
Al_2O_3	<0.02		0.05	0.06	<0.02	0.03	<0.02	<0.02	<0.02	<0.02
Cr_2O_3	<0.05		<0.05		1.11	0.79	0.53	0.10	0.16	0.20
MgO	<0.02		0.04	0.03	0.05	<0.02	<0.02	12.16	5.28	2.34
MnO	<0.03		<0.03		<0.03	<0.03	<0.03	0.27	0.81	2.14
FeO*	0.21	0.14	0.26	0.09	0.67	<0.1	<0.1	28.85	38.37	40.73
	99.39	0.90	99.51	1.09	99.27	98.87	99.05	99.17	99.84	99.22
0=	6		4		2	2	2	3	3	3
Nb					0.003					
Ta										
Si			1.050	0.009	0.001				0.001	0.001
Ti	2.002	0.017	0.002	0.002	0.978	0.981	0.985	1.006	1.004	1.004
Zr	0.984	0.014	0.930	0.011	0.004	0.012	0.009			
Hf	0.007	0.001	0.012	0.002	0.000	0.000				
Al			0.002	0.002	0.000	0.001				
Cr					0.012	0.008	0.006	0.002	0.003	0.004
Mg			0.002	0.001				0.420	0.191	0.087
Mn								0.005	0.017	0.045
Fe*	0.008	0.006	0.006	0.002	0.008			0.559	0.777	0.848
	3.002	0.003	2.004	0.001	1.006	1.002	1.000	1.991	1.992	1.989
Ti/Zr	2.03	0.05								

Notes: Numbers next to S.D. no. mean standard deviation and number of analyses. FeO* = total iron as FeO, Fe* = total iron as Fe.

TABLE 1. —*CONTINUED*

Gabbro				
cpx		opx		phl
avg	std no. 4	avg	std no. 5	R15-4-28
52.85	0.27	56.93	0.41	40.19
1.27	0.13	0.50	0.14	4.99
2.67	0.10	1.01	0.05	14.29
0.71	0.17	0.08	0.04	0.25
3.30	0.30	7.18	0.31	4.20
0.11	0.03	0.20	0.02	0.01
17.28	0.72	33.47	0.30	21.88
21.50	0.86	1.11	0.24	0.00
0.67	0.05	0.02	0.01	1.40
0.02		0.00		8.19
0.05		0.07		0.16
100.43	0.57	100.57	0.64	95.56
6		6		22
1.916	0.003	1.966	0.007	5.658
0.035	0.003	0.013	0.004	0.529
0.114	0.004	0.041	0.002	2.371
0.020	0.005	0.002	0.001	0.027
0.100	0.009	0.207	0.008	0.494
0.003	0.001	0.006	0.000	0.001
0.933	0.038	1.721	0.021	4.590
0.835	0.033	0.041	0.009	0.000
0.047	0.004	0.002	0.001	0.381
0.001		0.000		1.471
0.001		0.002		0.019
4.006	0.003	4.001	0.005	15.540
0.903	0.006	0.893	0.005	0.903
0.151	0.029	0.052	0.022	0.011

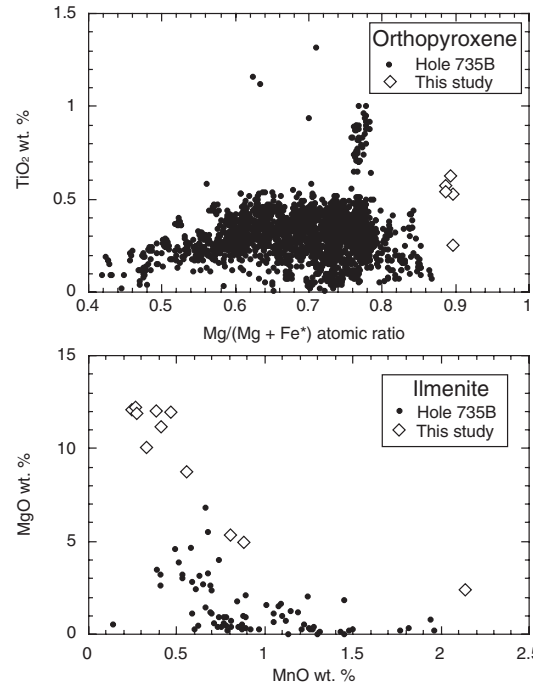

FIGURE 5. Comparisons of mineral compositions from the gabbroic vein and the gabbros from Hole 735B. (**a**) Mg' [=Mg/(Mg + Fe*) atomic ratio: Fe* = total iron as Fe] vs. wt% TiO_2 of orthopyroxene. Orthopyroxene compositions in the gabbros of Hole 735B are from Dick et al. (2002). (**b**) wt% MgO vs. wt% MnO of ilmenite. Ilmenite compositions in the gabbros of Hole 735B are from Natland et al. (1991), Hébert et al. (1991), Hertogen et al. (2002), and Niu et al. (2002)

Gabbroic vein

Clinopyroxene is magnesian with a Mg' of 0.90. The TiO_2, Al_2O_3, Cr_2O_3, and Na_2O contents of clinopyroxene are 1.3, 2.7, 0.7, and 0.7 wt%, respectively. Orthopyroxene is also magnesian with a Mg' of 0.89 (Fig. 5a). The Al_2O_3, Cr_2O_3, and TiO_2 contents are 1, <0.15, and 0.3–0.6 wt%, respectively. Ilmenite exhibits a wide range in MgO and MnO from 2 to 12 wt% and from 0.3 to 2 wt%, respectively. The MgO contents of ilmenite increase as the MnO contents decrease (Fig. 5b). The ZrO_2 and Cr_2O_3 contents of rutile ranges from 0.3 to 1.8 wt% and from 0.2 to 1 wt%, respectively (Fig. 6). Rutile contains up to 0.5 wt% Nb_2O_5 and occurs near to and/or associated with zircon grains. The compositions of zircon are uniform for different grains. The HfO_2 contents of zircon is 1.4 wt%. A Zr/Ti ratio of srilankite is close to a stoichiometric value of one-half ($Ti_{2.00}Zr_{0.98}Hf_{0.01}Fe_{0.01}O_6$) (Table 2). The HfO_2 and FeO contents of srilankite are 0.5 and 0.2 wt%, respectively.

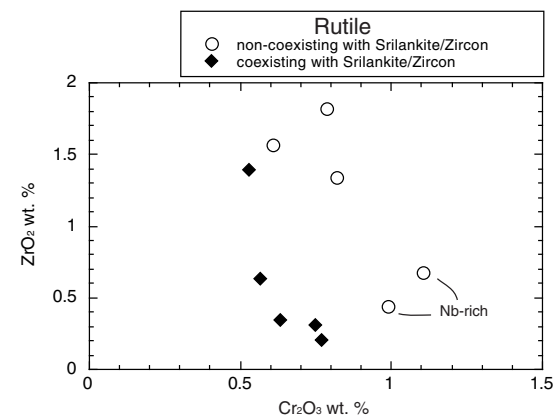

FIGURE 6. wt% Cr_2O_3 vs. wt% ZrO_2 of rutile in the gabbroic vein.

DISCUSSION

Origin of srilankite: metamorphic or magmatic?

The phase relationships in the system ZrO_2-TiO_2 have been investigated experimentally (McHale and Roth 1986; Willgallis et al. 1987). McHale and Roth (1986) found Ti_2ZrO_6 as the stable phase occurring in the system ZrO_2-TiO_2 at a pressure of 1 atm and a temperature of <1100 °C, with a small range of Zr/Ti ratio. In the studied sample, as well as other localities (Willgallis et al. 1983; Wang et al. 1999; Bingen et al. 2001), the Zr/Ti ratio of srilankite is close to one-half, but that from Yagodka varies significantly from 0.42 to 0.57 (Kostrovitskiy et al. 1993). The compositions of the srilankite from Yagodka were, however, calculated with a correction for the matrix interference because the srilankite was too small to analyze.

Willgallis et al. (1987) synthesized srilankite at 128–635 °C and 0.15–3.0 kbar under hydrothermal conditions. Based on their experimental results, they proposed that srilankite is of hydrothermal origin because they found srilankite in pebbles, mainly consisting of zirconolite and baddeleyite with lesser amounts of geikielite, spinel, and perovskite, in the washing concentrate of

a gemstone mine in Sri Lanka (Willgallis et al. 1983). However, srilankite also has been found as inclusions in garnets, which may represent the deep mantle sampled by lamprophyre pipes and ultramafic diatremes (Kostrovitskiy 1993; Wang et al. 1999). Wang et al. (1999) estimated that garnet containing srilankite inclusions were formed at 1.5–3 GPa and 600–800 °C along the local ancient geotherm. It is, therefore, apparent that hydrothermal activity at low-temperature conditions is not always necessary for the formation of srilankite. Despite intense alteration under low-temperature conditions in the studied sample, the srilankite we studied locally is included completely in magmatic ilmenite-rutile intergrowths where other phases and cracks do not exist (Figs. 3b, 3c).

Bingen et al. (2001) reported srilankite in mafic granulites, for which *P-T* estimates of <1 GPa and 800–850 °C had been made previously (Austrheim and Griffin 1985). Because the srilankite they found is always situated between baddeleyite and ilmenite (when baddeleyite occurs with srilankite), they concluded that the srilankite was formed under granulite-facies conditions by the reaction:

$$2ZrO_2 \text{ (baddeleyite)} + 4FeTiO_3 \text{ (in ilmenite)} + O_2 = 2Ti_2ZrO_6 \text{ (srilankite)} + 2Fe_2O_3 \text{ (in ilmenite)}.$$

Baddeleyite actually has been reported in gabbroic rocks (Keil and Fricker 1974; Batiza and Vanko 1985; Naslund 1987; Ross and Elthon 1997) and is also found in the gabbros of Hole 735B (J. Maeda, unpublished data). Baddeleyite could have formed either as an exsolution product from ilmenite (Batiza and Vanko 1985; Naslund 1987; J. Maeda, unpublished data) or as a late-stage phase crystallizing from melts (Keil and Fricker 1974; Ross and Elthon 1997). The srilankite in the gabbroic vein does not exhibit a readily recognizable reaction relationship with a former baddeleyite. Moreover, we cannot find any reaction textures between zircon, which is another possible source for Zr, and other minerals in the studied sample. The presence of discrete zircon grains indicates that the melts producing the gabbroic vein should be oversaturated with ZrO_2. The ZrO_2 contents of rutile may tend to be high in srilankite-free and zircon-free grains, but not so distinctive. There are no systematic differences in the chemistry of ilmenite between srilankite-bearing and srilankite-free grains. From these lines of evidence, we propose that the srilankite in the studied sample crystallized with rutile and ilmenite from melts rather than by metamorphic recrystallization after the formation of the vein.

Evolution of a melt from which srilankite was crystallized: implications for peridotite-melt interactions

Many gabbroic rocks have been collected by dredging and drilling from or near the Atlantis II Fracture Zone (e.g., Bloomer et al. 1989; Dick et al. 2000; Coogan et al. 2001; Natland and Dick 2001). The gabbros have been divided mainly into two major types: (1) oxide-poor olivine gabbros, and (2) Fe-Ti-rich oxide-gabbro (e.g., Bloomer et al. 1989; Dick et al. 2000). The former and the latter gabbros are distributed irregularly throughout the section of Hole 735B, although oxide-gabbros are more abundant in the upper 500 m (Dick et al. 2000). The mineralogical variations of these gabbros and the intrusive contact relationships suggest that the Fe-Ti-rich melts producing the oxide-gabbros were derived from late magmatic liquids squeezed from the mesostasis of crystallizing olivine gabbros intrusions (e.g., Bloomer et al. 1989; Dick et al. 2000; Natland and Dick 2001). There is convincing evidence for local migration and intrusion of Fe-Ti-rich melts along shear zones throughout the olivine gabbros during deformation (e.g., Dick et al. 2000).

Petrographic characteristics of the gabbroic vein such as the presence of granular orthopyroxene rather than interstitial orthopyroxene, zircon, and apatite indicate that the gabbroic vein was formed from late melts (Dick et al. 2000). This finding is consistent with the observation that ilmenite and magnetite usually appear on the liquidus of fractionated high Ti-Fe melts only after about 90% crystallization at low-pressure conditions (Clague et al. 1981; Juster et al. 1989).

Veins of evolved gabbros cutting abyssal peridotites have been observed from slow-spreading ridges (Fisher et al. 1986; Bloomer et al. 1989; Mével et al. 1991; Cannat et al. 1992) as well as from fast-spreading ridges (e.g., Constantin 1999). Bloomer et al. (1989) suggested the possibility that a fractionated gabbroic vein cutting peridotite from the SWIR resulted from downward intrusion of late magmatic melts formed from the crystallizing olivine gabbro cumulate. In the studied sample, the gabbro vein apparently obliquely cuts the igneous layering structure of peridotite, suggesting that the timing of intrusion of the gabbro vein was later than the formation of the dunite. However, the gabbroic vein studied clearly has features that indicate geochemical interaction with the peridotite host, indicating that the peridotite was still hot enough to sustain peridotite-melt interaction, although the chemical exchanges only affected minerals located within a few centimeters of the gabbroic vein. Moreover, Ti-Fe-rich oxide gabbros markedly diminish in volume downward in Hole 735B (e.g., Dick et al. 2000). We favor the idea that the gabbroic vein studied was formed as an in-situ highly fractionated melt from a MORB-type melt during ascent in the

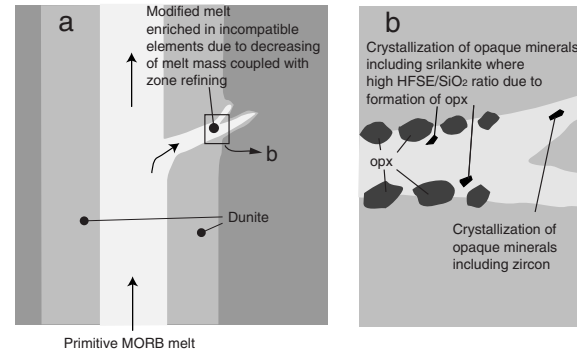

FIGURE 7. Schematic model showing the melt-mantle interactions. (**a**) The formation of a modified melt due to interaction between lherzolite and a primary MORB melt resulting in the formation of dunite as a melt conduit. The modified melt was enriched in incompatible elements due to decreasing of melt mass coupled with a zone-refining effect. See text for more details. (**b**) The precipitation of srilankite from the modified melt. Srilankite might be formed locally in high $HFSE/SiO_2$ areas where orthopyroxenes (opx) were formed by interaction with host peridotite and the modified melt.

uppermost mantle.

A parental melt for the formation of the studied gabbroic vein would be similar to that for the gabbros of Hole 735B. However, orthopyroxenes in the gabbroic vein have distinctive chemical characteristics compared with those in the gabbros of Hole 735B (Fig. 5a). In addition to this, many ilmenite grains in the gabbroic vein are distinctively high in MgO compared with those in the gabbros of Hole 735B (Fig. 5b). Thus, the chemical characteristics of minerals in the gabbroic vein are different from those in both the oxide-gabbros and olivine-gabbros of Hole 735B. Those aspects of mineral compositions, coupled with presence of phlogopite, can be interpreted to reflect high MgO, high Cr_2O_3, high HFSE, high K_2O, and high H_2O abundances in the melts. On the other hand, the TiO_2 enrichment of spinel (Fig. 4) and clinopyroxene in the peridotite host in contact with the gabbroic vein may result from the involvement of Ti-rich melts in the peripheral region of the interaction.

Melts formed by the partial melting of peridotite may change their compositions during ascent (Kushiro 1968; Kelemen 1986; Arai et al. 1997). The effect of interaction of peridotite with basaltic melt is to produce melts that are more enriched in Mg and incompatible trace elements than melts produced by crystal fractionation alone (Kelemen 1986; Arai et al. 1997). Primary MORB melts produced in the deeper part of the upper mantle should react with shallower mantle peridotite and selectively dissolve orthopyroxene with the simultaneous crystallization of olivine resulting in the formation of dunite as a melt conduit (Kelemen et al. 1995; Arai et al. 1997) (Fig. 7a). Chromium may be supplied to the melt from orthopyroxene in this stage. During melt transport processes, decreasing melt mass coupled with the zone-refining effect (Harris 1957; Kushiro 1968) resulted in effective enrichment of HFSE and other incompatible elements such as K_2O and H_2O in modified melts, particularly in a small conduit (Fig. 7). We propose that srilankite may have been precipitated from such modified melts.

Loferski and Arculus (1993) reported multiphase inclusions consisting of clinopyroxene + ilmenite + apatite with a minor amount of baddeleyite (ZrO_2) within cumulus plagioclase grains from anorthosites of the Stillwater Complex, Montana. Because the inclusions are multiphase and all consist of the same assemblage, the authors suggested that the multiphase inclusions originated as liquid droplets rather than solid aggregates at the time of their entrapment in the plagioclase. They proposed that the multiphase inclusions were crystallized from an unusual liquid enriched in HFSE, REE, P, Fe, and Mg relative to the bulk of the anothosite, which was formed by silicate liquid immiscibility. Ross and Elthon (1997) reported baddeleyite in the recovered cores of gabbroic rock at Sites 921 through 924 during Leg 153 of ODP (the western wall of the median valley of the Mid-Atlantic Ridge south of the Kane Fracture Zone). They suggested that the baddeleyite formed as an exsolution product from ilmenite, as a late-stage crystallizing phase from trapped melts, or by crystallization from melts enriched in Zr, P, and Fe, which had formed by liquid immiscibility of very evolved intercumulus melt. However, liquid immiscibility is not a viable explanation for the origin of a unique melt that produced the srilankite in the gabbroic rock studied here because the formation of srilankite might be controlled by local differences in HFSE/SiO_2 and by Zr/Ti ratios in the melt as discussed next.

The occurrence of srilankite in the gabbroic vein is thought to be anomalous, because it is expected that evolved melts will ultimately crystallize zircon, not srilankite. The question of crystallization of srilankite from evolved melts now can be considered. The distribution of srilankite and zircon is heterogeneous, even on a thin-section scale. The SiO_2 contents of evolved melts might be locally low, where HFSE/SiO_2 is high enough to crystallize srilankite. One plausible explanation for the local heterogeneity in SiO_2 contents in evolved melts is that the crystallization of orthopyroxene, due to interaction of SiO_2-component in evolved melts with olivine in peridotite hosts, locally will decrease SiO_2 contents but not incompatible elements in the evolved melts, particularly near the peridotite hosts (Fig. 7b). This scenario is consistent with the observation that srilankite is found in an area rich in orthopyroxene grains, i.e., close to the margin of the vein.

If the magma supply is high, like beneath fast-spreading ridges, evolved melts will be mixed with subsequently supplied more primitive melts. In such a case, crystallization of chromian spinel will occur because the mixed magma is expected to be oversaturated with chromian spinel (Irvine 1977; Zhou et al. 1994; Arai and Yurimoto 1994; Arai and Matsukage 1998). Arai et al. (1997) suggested that melt-mantle interaction seems more effective within melt-stagnant or failed conduits because the melt can be evolved through interaction without mixing with primitive magmas. Dunites, probably marking melt-flow channels through the mantle, are rare from the SWIR transforms, including the Atlantis II Fracture Zone (Dick 1989; Dick et al. 1991). This observation suggests that there might be little melt transport in the shallow mantle at the Atlantis II Fracture Zone. Thus, we conclude that srilankite is crystallized locally from modified melts due to peridotite-melt interactions in a region with a low rate of magma supply, i.e., slow-spreading ridges.

ACKNOWLEDGMENTS

We are grateful to Captain Ishida and the crew of the Yokosuka as well as the Shinkai team who contributed to the success of the ABCDE cruise. We thank the other participants to the cruise, H. Kumagai, M. Cheadle, B. John, Y. Otomo, A. Kvassnes, G. Baines, A. Hamadate, M. Imamura, E. Miranda, and J. Warren, for their help in collecting the data and fruitful discussions on board. T.M. deeply thanks S. Arai for his discussions on peridotite-melt interactions, and K. Tazaki for EPMA analysis at Kanazawa University. The constructive reviews by K. Righter and J.C. Ayers improved the manuscript. Support for this work was provided by the JAMSTEC.

REFERENCES CITED

Arai, S. and Matsukage, K. (1998) Petrology of a chromitite micropod from Hess Deep, equatorial Padific: a comparison between abyssal and alpine-type podiform chromitites. Lithos, 43, 1–14.

Arai, S. and Yurimoto, H. (1994) Podiform chromitites of the Tari-Misaka ultramafic complex, Southwestern Japan, as mantle-melt interaction products. Economic Geology, 89, 1279–1288.

Arai, S., Inoue, T., and Oyama, T. (1988) Igneous petrology of the Ochiai-Hokubo ultramafic complex, the Sangun zone, western Japan: a preliminary report. Journal of Geological Society of Japan, 94, 91–102. (in Japanese with English abstract)

Arai, S., Matsukage, K., Isobe, E., and Vysotskiy S. (1997) Concentration of incompatible elements in oceanic mantle: Effect of melt/wall interaction in stagnant or failed melt conduits within peridotite. Geochimica et Cosmochimica Acta, 61, 671–675.

Austrheim, H and Griffin, W.L. (1985) Shear deformation and eclogite fromation within granulite-facies anorthosites of the Bergen Arcs, western Norway. Chemical Geology, 50, 267–281.

Batiza, R. and Vanko, D.A. (1985) Petrologic evolution of large failed rifts in the Eastern Pacific: petrology of volcanic and plutonic rocks from the Math-

ematician Ridge Area and the Guadalupe Trough. Journal of Petrology, 26, 564–602.

Bingen, B. Austrheim, H., and Whitehous, M. (2001) Ilmenite as a source for zirconium during high-grade metamorphism? Textural evidence from the Caledonides of Western Norway and implications for zircon geochronology. Journal of Petrology, 42, 355–375.

Bloomer, S.H., Natland, J.H., and Fisher, R.L. (1989) Mineral relationships in gabbroic rocks from fracture zones of Indian Ocean ridges: evidence for extensive fractionation, parental diversity and boundary-layer recrystallization. In A.D. Saunders and M.J. Norry, Eds., Magmatism in the Ocean Basins, Geological Society Special Publication No.42, pp. 107–124.

Bown, J.W. and White, R.S. (1994) Variation with spreading rate of oceanic crustal thickness and geochemistry. Earth and Planetary Science Letters, 121, 435–449.

Cannat, M., Bideau, D., and Bougault, H. (1992) Serpentinized peridotites and gabbros in the Mid-Atlantic Ridge axial valley at 15°37'N and 16°52'N. Earth and Planetary Science Letters, 109, 87–106.

Clague, D.A., Frey, F.A., Thompson, G., and Rindge, S. (1981) Minor and trace element geochemistry of volcanic rocks dredged from the Galapagos Spreading Center Role of crystal fractionation and mantle heterogeneity. Journal of Geophysical Research, 86, 9469–9482.

Constantin, M. (1999) Gabbroic intrusions and magmatic metasomatism in harzburgites from the Garret transform fault: implications for the nature of the mantle-crust transition at fast-spreading ridges. Contributions to Mineralogy and Petrology, 136, 111–130.

Coogan, L.A., MacLeod, C.J., Dick, H.J.B., Edwards, S.J., Kvassnes, A., Natland, J.H., Robinson, P.T., Thompson, G., and O'Hara, M.J. (2001) Whole-rock geochemistry of gabbros from the Southwest Indian Ridge: constraints on geochemical fractionations between upper and lower oceanic crust and magma chamber processes at (very) slow-spreading ridges. Chemical Geology, 178, 1–22.

Dick, H.J.B. (1989) Abyssal peridotites, very slow spreading ridges and ocean ridge magmatism. In A.D. Saunders and M.J. Norry, Eds., Magmatism in the Ocean Basins, Geological Society Special Publication, 42, 71–105.

Dick, H.J.B., Schouten, H., Meyers, P.S., Gallo, D.G., Bergh, H., Tyce, R., Patriat, P., Johnson, K. T.M., Show, J., and Fisher, A. (1991) Tectonic evolution of the Atlantis II Fracture Zone. Proceedings of the Ocean Drilling Program, 118, 359–398. College Station, Texas.

Dick, H.J.B., Natland, J.H., Alt, J.C., Bach, W., Bideau, D., Gee, J.S., Haggas, S., Hertogen, J.G.H., Hirth, G., Holm, P.M., Ildefonse, B., Iturrino, G.J., John, B.E, Kelley, D.S., Kikawa, E., Kingdon, A., LeRux, P.J., Maeda, J., Meyer, P.S., Miller, D.J., Naslund, H.R., Niu, Y-L., Robinson, P.T., Snow, J., Stephen R.A., Trimby, P.W., Worm H-U., and Yoshinobu A. (2000) A long in situ section of the lower ocean crust: results of ODP Leg 176 drilling at the Southwest Indian Ridge. Earth and Planetary Science Letters, 179, 31–51.

Dick, H.J.B., Ozawa, K., Meyer, P.S., Niu, Y., Robinson, P.T., Constantin, M., Hebert, R., Natland, J.H., Hirth, J.G., and Mackie, S.M. (2002) Primary silicate mineral chemistry of a 1.5-km section of very slow spreading lower ocean crust: ODP Hole 735B, Southwest Indian Ridge. In J.H. Natland, H.J.B. Dick, D.J. Jiller and R.P. Von Herzen, Eds., Proceedings of the Ocean Drilling Program, Science Results, 176, 1–60 (on line). Available at http://www-odp.tamu.edu/publications/176 SR/VOLUME/CHAPTERS/SR176 10.PDF.

Fisher, R.L., Dick, H.J.B., Natland, J.H., and Meyer, P.S. (1986) Mafc/ultramafic suites of the slowly spreading Southwest Indian Ridge: Protea exploration of the Antarctic Plate Boundary, 24°E-47°E, 1984. Ophioliti, 11, 147–178.

Harris, P.G. (1957) Zone refining and the origin of potassic basalts. Geochimica et Cosmochimica Acta, 12, 195–208.

Hébert, R., Constantin, M., and Robinson, P.T. (1991) Primary mineralogy of Leg 118 gabbroic rocks and their place in the spectrum of oceanic mafic igneous rocks. Proceedings of the Ocean Drilling Program, 118, 3–20. College Station, Texas.

Hertogen, J., Emmermann, R., Robinson, P.T., and Erzinger, J. (2002) Lithology, mineralogy, and geochemistry of the lower ocean crust, ODP Hole 735B, Southwest Indian Ridge. In J.H. Natland, H.J.B. Dick, D.J. Miller, and R.P. Herzen, Eds., Proceedings of the Ocean Drilling Program, Scientific results, 176, 1–82 (Online). Avilable at <http://www-odp.tamu.edu/publications 176/SR/VOLUME/CHAPTERS/SR176 06.PDF>.

Hosford, A., Tivey, M., Matsumoto, T., Dick, H.J.B., Schouten, H., and Kinoshita, H. (2003) Crustal magnetization and accretion at the Southwest Indian Ridge near the Atlantis II fracture zone, 0-25Ma, Journal of Geophysical Research, 108, 2169–2191.

Juster, T.C., Grove, T.L., and Perfit, M.R. (1989) Experimental constraints on the generation of Fe-Ti basalts, andesites and rhyodacites at the Galapagos Spreading Center, 85°W and 95°W. Journal of Geophysical Research, 94, 9215–9247.

Keil, K. and Fricker, P.E. (1974) Baddeleyite (ZrO_2) in gabbroic rocks from Axel Heiberg Island, Canadian Arctic Archipelago, American Mineralogist, 59, 249–253.

Kelemen, P.B. (1986) Assimilation of ultramafic rock in subduction-related magmatic arc. Journal of Geology, 94, 829–843.

Kelemen, P.B., Shimizu, N., and Salters, V.J.M. (1995) Extraction of mid-ocean-ridge basalt from the upwelling mantle by focused flow of melt in dunite channels. Nature, 375, 747–753.

Kostrovitskiy, S.I., Garanin, V.K., and Varlamov, D.A. (1993) A second occurrence of srilankite. Transactions of the Russian Academy of Sciences, 329A, 133–137.

Kushiro, I. (1968) Compositions of magmas fromed by partial zone melting in the earth's upper mantle. Journal of Geophysical Research, 73, 619–634.

Loferski, P.J. and Arculus, R.J. (1993) Multiphase inclusions in plagioclase from anorthosites in the Stillwater Complex, Montana: implications fro the origin of the anorthosites. Contributions to Mineralogy and Petrology, 114, 63–78.

McHale, A.E and Roth, R.S. (1986) Low-temperature phase relationships in the system ZrO_2-TiO_2. Journal of the American Ceramic Society, 69, 827–832.

Mével, C., Cannat, M., Gente, P., Marion, E., Auzende, J.M. and Karson, J.A. (1991) Emplacement of deep crustal and mantle rocks on the west median valley wall of the MARK area (MAR, 23 °N). Tectonophysics, 190, 31–53.

Muller, M.R., Robinson, C.J., Minshull, T.A., White, R.S., and Bickle, M.J. (1997) Thin crust beneath ocean drilling program borehole 735B at the Southwest Indian Ridge? Earth and Planetary Science Letters, 148, 93–107.

Naslund, H.R. (1987) Lamellae of baddeleyite and Fe-Cr-spinel in ilmenite from the Basistoppen Sill, East Greenland. Canadian Mineralogist, 25, 91–96.

Natland, J.H. and Dick, H.J.B. (2001) Formation of the lower ocean crust and the crystallization of gabbroic accumulates at a very slowly spreading ridge. Journal of Volcanology and Geothermal Research, 110, 191–233.

Natland, J.H., Meyer, P.S., Dick, H.J.B., and Bloomer, S.H. (1991) Magmatic oxides and sulfides in gabbroic rocks from Hole 735B and the later development of the liquid line of descent. Proceedings of the Ocean Drilling Program, 118, 75–111. College Station, Texas.

Niu, Y., Gilmore, T., Mackie, S., Greig, A., and Bach, W. (2002) Mineral chemistry, whole-rock compositions, and petrogenesis of Leg 176 gabbros: data and discussion. In J.H. Natland, H.J.B. Dick, D.J. Jiller, and R.P. Von Herzen, Eds., Proceedings of the Ocean Drilling Program, Scientific Results, 176, 1–60 (on line). Available at http://www-odp.tamu.edu/publications/176 SR/VOLUME/CHAPTERS/SR176 08.PDF

Ross, K. and Elthon, D. (1997) Cumulus and postcumulus crystallization in the oceanic crust: major- and trace-element geochemistry of Leg 153 gabbroic rocks. In J.A. Karson, M. Canat, D.J. Miller, and D. Elthon, Eds., Proceedings of the Ocean Drilling Program, Scientific Results, 153, 333–350.

Wang, L., Essene, E.J., and Zhang, Y. (1999) Mineral inclusions in pyrope crystals from Garnet Ridge, Arizona, USA: implications for processes in the upper mantle. Contributions to Mineralogy and Petrology, 135, 164–178.

Willgallis, A., Siegmann, E., and Hettiaratch, T. (1983) Srilankite, a new Zr-Ti oxide mineral. Neues Jahrbuch für Mineralogie, Monatshefte, H4, 151–157.

Willgallis, A., Brauer, R., and Buhl, J-C. (1987) Investigation regarding the synthesis of srilankite ($Zr_{0.33}Ti_{0.67})O_2$. Neues Jahrbuch für Mineralogie. Monatshefte, H3, 129–135.

Zhou, M.-F., Robinson, P.T., and Bai, W.-J. (1994) Formation of podiform chromitites by melt/rock interaction in the upper mantle. Mineralium Deposita, 29, 98–101.

MANUSCRIPT RECEIVED MAY 6, 2003
MANUSCRIPT ACCEPTED DECEMBER 5, 2003
MANUSCRIPT HANDLED BY KEVIN RIGHTER